

# Two Dimensional Compressed Sampling Reconstruction of Hyperspectral Images based on Spectral Prediction

Li Wang, Wei Wang, Boni Liu

Department of Electronic Engineering, Xi'an Aeronautical University, Xi'an Shaanxi 710077, China.

---

## Abstract

The development of compressive techniques of hyperspectral images (HSI) becomes critical due to the limitations of the requirements of data storage, transmission and processing. Recently, Compressed Sampling (CS) has been used for hyperspectral imaging for its ability to recover the original data exactly under certain condition at a much lower sampling rate than Nyquist rate. In this paper, a residual reconstruction algorithm incorporating with two dimensional compressed sampling (2DCS) for Hyperspectral images is proposed to improve the performance of reconstruct algorithm. In the reconstruction process, spectral prediction is introduced for the strong spectral correlation between hyperspectral image bands. The experimental results reveal that the proposed technique achieves significantly higher quality than a straightforward reconstruction that reconstructs the hyperspectral images band by band independently. Meanwhile, the comparison between 2DCS and block-based compressed sampling (BCS) is developed and the results demonstrate that the superiority of 2DCS over BCS is in terms of high PSNR with respect to sampling rate.

## Keywords

Hyperspectral images, Two dimensional compressed sampling, Spectral prediction, PSNR.

---

## 1. Introduction

Hyperspectral images contain rich two-dimensional spatial geometric information and one-dimensional spectral information, which are suitable for the fields of target detection and recognition, image classification, etc. [1]-[6]. The resultant large volume of data collected by such sensors constitutes great challenges to computer processing, storage and transmission. For instance, an image scene acquired by the Airborne Visible/Infrared imaging Spectrometer (AVIRIS) consists of about 140 MB. That is why the compression of hyperspectral images (HSI) becomes more and more urgent, particularly for those images that are to be transmitted directly to the ground and distributed to users. The traditional compressive algorithms have high-complexity encoders, poor error-resilient performance, and the computational complexity is exponential growing with the dimension of image increasing, which are not suitable for the application of hyperspectral images.

Recent years have seen significant interest in the paradigm of compressed sensing (CS) [7]-[9] which permits, under certain conditions, signals to be sampled at sub-Nyquist rates via linear projection onto a random basis while still enabling exact reconstruction of the original signal. Due to the simplicity and easy implementation of the measurement process at the sampling process, the CS framework is a natural fit for hyperspectral image compression, which requires low complexity encoding and could solve the difficulty of storage and transmission effectively.

When using CS theory in the compressed of hyperspectral images [10]-[13], one of the primary challenges is the large computational cost typically associated with reconstruction from incomplete sampled data and the other challenge is how to improve the quality of reconstructed image via making use of the characteristic of hyperspectral images. In the existing reconstruction algorithms, most methods reconstruct the images band by band independently without considering the correlation between adjacent bands. In literature [14], a reconstruction algorithm based on interband prediction and joint optimization is proposed to use linear prediction to remove the correlations among successive bands. Distributed CS [15] uses the reconstructed bands as edge information to improve other bands. Three-dimensional CS has been adapted to hyperspectral images to decrease the spectral correlation [16]. A compressed sensing projection and reconstruction algorithm for hyperspectral images which utilizes the spatial correlation and spectral correlation is proposed in [17], and the algorithm shows higher reconstruction quality images as well as lower coding complexity.

Fowler proposed a simple block-based CS (BCS) reconstruction [18] incorporating considering the motion estimation and compensation to improve the reconstruct quality. But the drawback of BCS is typically a reduced quality of image reconstruction, so how to improve the reconstruct algorithm and reduce the computational burden is the focus because the performance of the reconstruct algorithm determines the quality of the reconstructed image and the quality of reconstructed image influences the application of HSI. In this paper, we are dedicated to improve the performance of reconstruct algorithm via taking advantage of spectral correlation between adjacent bands of HSI.

This paper is organized as follows. Section 2 presents the principle theory of compressed sensing, the simple measurement method and recovery problem are described. Section 3 develops the proposed reconstruction method. Firstly, the two dimensional compressed sampling method is presented. Then the framework of the proposed method is given and the steps of residual reconstruction are listed with introducing spectral prediction. The experimental results are given in Section 4 to test the performance of the reconstruct algorithm and section 5 gives the concluding remarks.

## 2. Principle Theory of Compressed Sampling

In brief, the new field of compressed sensing has given us a fresh look at data acquisition, one of the fundamental tasks in signal processing. The message of this theory can be summarized succinctly: the number of measurements we need to reconstruct a signal depends on its sparsity rather than its bandwidth. The core idea of compressed sensing is that if a signal or image of interest is sparse or compressible in some domain, then it can be reconstructed accurately from very few (relative to the dimension of the signal or image) non-adaptive measurements. More specifically, suppose that we want to recover real-valued signal  $x$  with length  $N$  from  $M$  samples such that  $M \ll N$ . In other words, we want to recover  $x$  from:

$$y = \Phi x \quad (1)$$

Where,  $y$  is the measurement value, its length is  $M$ , and  $\Phi$  is an  $M \times N$  measurement matrix with sampling rate, or subrate, being  $SR = M/N$ .

Recovering  $x$  from  $y$  is then a linear inverse problem. Because of the number of unknowns is much larger than the number of observations, the equation is underdetermined, so recovering every  $x \in R^N$  from its corresponding  $y \in R^M$  is impossible in general. However, if  $x$  is sufficiently sparse or compressive in some domain, several methods for recovering sparse  $x$  from the limited number of measurements have been proposed. Here, we only give one example of solving this problem. The above problem can be transformed into a minimum  $l_0$  norm optimization problem.

$$\hat{x} = \arg \min \|x\|_0 \quad \text{subject to} \quad y = \Phi x \quad (2)$$

There are several issues that arise when the signal  $x$  is an image. From the perspective of practical implementation, the dimensionality of the measurement matrix in equation (1) grows very quickly as the size of image  $x$  increases due to the multidimensional nature of image data. This leads to a huge memory required to store the sampling operator when  $\Phi$  is implemented as a matrix within the CS

sensing process. Additionally, a large  $\Phi$  yields a huge memory and computational burden within the CS reconstruction process. Meanwhile, the reconstruct performance effects the compressed sampling of HSI. Therefore, when using CS for hyperspectral images, how to look for an appropriate sampling matrix and a high performance reconstruct algorithm is the critical issue.

In fact, there are many measurement matrices, such as gauss matrix, Bernoulli matrix, partial Fourier matrix, Toeplitz matrix and others. However, these matrices are random and could not be applied to the actual system. In order to solve this problem, we introduce the circulant sampling (CirS) to replace a random sampling ensemble with the advantages of easy hardware implementation, memory efficiency and fast decoding. It has been shown that CirS is competitive with random sampling in terms of recovery accuracy [19]. In the previous work [16], three dimensional compressed sampling (3DCS) method is proposed, in the sampling process, it considers the spatial and spectral correlation, so it needs large memory to store the sampling matrix. In this paper, two dimensional compressed sampling is used to save the memory requirement, and in the reconstruction process, spectral prediction is introduced to improve the reconstruct performance.

### 3. Proposed Reconstruct Algorithm

The architecture of the proposed algorithm is depicted in Figure 1, which makes use of the strong spectral correlation in the reconstruction process to improve the accuracy of the reconstruct algorithm. In the figure, all the basic formula are given and the procedures are clear. The figure introduces the proposed reconstruct algorithm using spectral prediction for residual reconstruction. In the framework, the hyperspectral images are sampled by 2DCS, and the bands are reconstructed by two dimensional total variation (2DTV) firstly. Then the residual reconstruct algorithm is applied using spectral prediction (SP) to improve the reconstruct performance. As shown in Figure 1,  $\mathbf{x}_k$  and  $\mathbf{x}_{k+1}$  represent the two adjacent bands, and are seen as key band and non-key band, respectively. In the sampling process,  $\mathbf{y}_k$  and  $\mathbf{y}_{k+1}$  are the measurements using 2DCS independently. In the reconstruction process, the key band and the non-key band are reconstructed by 2DTV independently and the result are  $\hat{\mathbf{x}}_k$  and  $\hat{\mathbf{x}}_{k+1}$ . Then the spectral correlation is utilized to improve the performance of non-key band. The predict value of the non-key band is the linear combination of the reconstructed  $\hat{\mathbf{x}}_k$  and the reconstructed  $\hat{\mathbf{x}}_{k+1}$ . Then the residual is calculated from the measurements of original data  $\mathbf{x}_{k+1}$  and the predict value  $\mathbf{x}_{k+1,sp}$ . The last step is obtaining the reconstructed residual result through 2DTV and revising the predict value. Note that, the symbol *iter* is the current iterative number, for the process is implemented in an iterative fashion. According to the spectral prediction and the sampling method, the proposed method is denoted as 2DCS-SP.

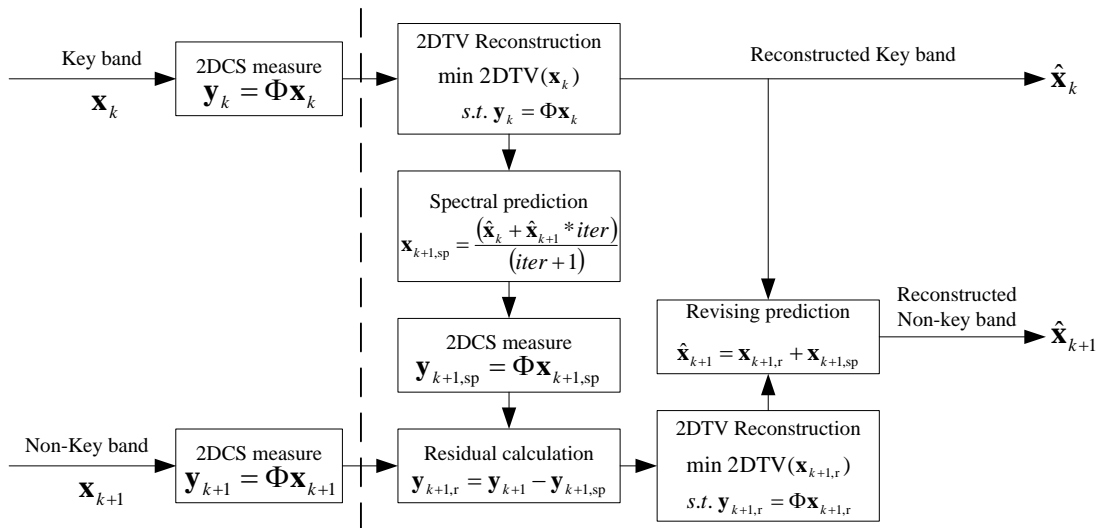


Figure 1. The architecture of proposed reconstruct algorithm.

### 3.1 Two Dimensional Compressed Sampling and Reconstruction

Hyperspectral images are often piecewise smooth in 2D spatial domain, and each spatial image is compressible. To fully exploit such rich compressibility, circulant sampling is introduced to replace random sampling matrix with the advantage of fast coding. The 2DCS [14][16] consists of random convolution and random subsampling. One band image  $\mathbf{x}_k$  convolves a random kernel  $\mathbf{H}$ , denoted by  $\mathbf{C}\mathbf{x}_k$ , where  $\mathbf{C}$  is the circulant matrix with  $\mathbf{H}$  as its first column.  $\mathbf{C}$  is diagonalized as  $\mathbf{C} = \mathbf{F}^{-1} \text{diag}(\hat{\mathbf{H}}) \mathbf{F}$ , where  $\hat{\mathbf{H}}$  is the Fourier transform of  $\mathbf{H}$ . Then the subsampling process is used on the  $\mathbf{C}\mathbf{x}_k$  by a random permutation ( $\mathbf{P}$ ) and a selecting factor  $\mathbf{S}_k$ . The final sampled data is expressed as  $\mathbf{B}_k = \mathbf{S}_k \mathbf{P} \mathbf{C} \mathbf{x}_k$ . Here,  $\mathbf{S}_k$  does not change with band and the sampling matrix is same for each band.

In 2D imaging CS, in order to use the piecewise smoothness in spatial domain, the total variation (TV) is often used to reconstruct the image from incomplete measurements. The widely-used form of TV is  $\text{TV}_{l_1, l_2}$ , however, the  $l_1$ -norm based TV measure is proven to be better than  $\text{TV}_{l_1, l_2}$  in reducing the sampling rate. According to the analyses above, the two dimensional total variation (2DTV) problem in this paper would be formulated as:

$$2\text{DTV}(\mathbf{x}_k) = \|\mathbf{D}_h \mathbf{x}_k\|_1 + \|\mathbf{D}_v \mathbf{x}_k\|_1. \quad (3)$$

Where,  $\mathbf{D}_h$  and  $\mathbf{D}_v$  are the horizontal and vertical gradient operators.

Thence, the reconstruct algorithm is to solve the following optimization problem:

$$\min_{\mathbf{x}_k} 2\text{DTV}(\mathbf{x}_k) \quad s.t. \quad \mathbf{S}_k \mathbf{P} \mathbf{C} \mathbf{x}_k = \mathbf{B}_k. \quad (4)$$

By introducing weight parameters  $\alpha_h = \alpha_v = 1$  and auxiliary parameters  $\mathbf{z} = (\mathbf{G}_h, \mathbf{G}_v, \mathbf{R})$ , Equation (3) could be employed in the form of Equation (5) as follows. This linearly constrained problem could be solved by augmented Lagrangian multipliers (ALM) [18] algorithm efficiently.

$$\begin{aligned} \min_{\mathbf{x}_k, \mathbf{G}_h, \mathbf{G}_v, \mathbf{R}} \quad & \alpha_h \|\mathbf{G}_h\|_1 + \alpha_v \|\mathbf{G}_v\|_1 \\ s.t. \quad & \mathbf{G}_h = \mathbf{D}_h \mathbf{x}_k, \mathbf{G}_v = \mathbf{D}_v \mathbf{x}_k, \mathbf{R}_k = \mathbf{C} \mathbf{x}_k, \mathbf{S}_k \mathbf{P} \mathbf{R}_k = \mathbf{B}_k \end{aligned} \quad (5)$$

### 3.2 Spectral Prediction

Unlike natural images, hyperspectral images have two spatial dimensional and one spectral dimensional information. So it has two types of correlations, namely: 1) spatial correlation and 2) spectral correlation. Among the existing methods, most of them have consider their spatial correlation to improve the performance of the sampling or reconstruct algorithm. But it may not be enough to independently apply CS theory to each band without exploiting the strong spectral correlation between hyperspectral images. The spectral correlation may be another class constraint in the recovery optimization problem. Specially, the spectral resolution in hyperspectral imaging is very high and could reach 10 nm. Therefore, in this paper, the non-key band could be predicted using the adjacent reconstructed band and is defined as:

$$\mathbf{x}_{k+1, sp} = (\hat{\mathbf{x}}_k + \hat{\mathbf{x}}_{k+1} * \text{iter}) / (\text{iter} + 1). \quad (6)$$

### 3.3 Residual Reconstruction

In this section, the residual reconstruct algorithm is described using one key and one non-key band as an example. It contains five steps, namely, spectral prediction, 2DCS measure, residual calculation, residual reconstruction and revising prediction.

Before the reconstruction process, the key and non-key bands should be measured by 2DCS firstly:

$$\mathbf{y}_k = \Phi \mathbf{x}_k. \quad (7)$$

$$\mathbf{y}_{k+1} = \Phi \mathbf{x}_{k+1}. \quad (8)$$

1) Spectral prediction: As mentioned before, the spectral prediction of  $\mathbf{x}_{k+1}$  is  $\mathbf{x}_{k+1, sp}$  obtained using equation (6). Before this prediction, the key band  $\mathbf{x}_k$  and the non-key band  $\mathbf{x}_{k+1}$  should be reconstructed first using 2DTV reconstruct algorithm.

2) 2DCS measure: The measurements of  $\mathbf{x}_{k+1,sp}$  is:

$$\mathbf{y}_{k+1,sp} = \Phi \mathbf{x}_{k+1,sp} . \quad (9)$$

3) Residual calculation: Calculate the residual between the measure of original non-key band and the predict value:

$$\mathbf{y}_{k+1,r} = \mathbf{y}_{k+1} - \mathbf{y}_{k+1,sp} . \quad (10)$$

4) Residual reconstruction: It is clear that  $\mathbf{y}_{k+1,r}$  is the random projection of the residual  $\mathbf{x}_{k+1,r}$ , between the original bands and the spectral prediction; i.e.,

$$\mathbf{y}_{k+1,r} = \mathbf{y}_{k+1} - \Phi \mathbf{x}_{k+1,sp} = \Phi(\mathbf{x}_{k+1} - \mathbf{x}_{k+1,sp}) = \Phi \mathbf{x}_{k+1,r} . \quad (11)$$

The recovery problem is written as:

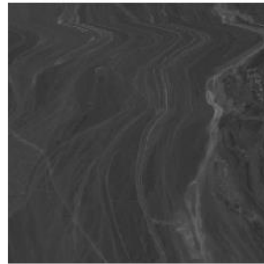
$$\min 2DTV(\mathbf{x}_{k+1,r}) \quad s.t. \quad \mathbf{y}_{k+1,r} = \Phi \mathbf{x}_{k+1,r} \quad (12)$$

5) Revising prediction. If the spectral prediction process is reasonably accurate, the residual  $\mathbf{x}_{k+1,r}$  should be much sparser than the original band  $\mathbf{x}_{k+1}$ ; 2DTV reconstruction should thereby be much more effective at recovering the residual  $\mathbf{x}_{k+1,r}$  from  $\mathbf{y}_{k+1,r}$  than it is at recovering  $\mathbf{x}_{k+1}$  from  $\mathbf{y}_{k+1}$ . Let  $\hat{\mathbf{x}}_{k+1,r}$  be the recovery from  $\mathbf{y}_{k+1,r}$ ; consequently, we can obtain an approximation reconstruction to  $\mathbf{x}_{k+1}$  as:

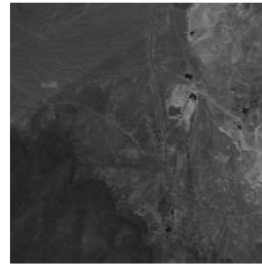
$$\hat{\mathbf{x}}_{k+1} = \hat{\mathbf{x}}_{k+1,r} + \mathbf{x}_{k+1,sp} . \quad (13)$$

## 4. Experimental Results

The performance of the proposed reconstruction algorithm is examined on two datasets from AVIRIS (<http://aviris.jpl.nasa.gov>). The images are cropped spatially to a small size, i.e., the rows and columns are 256. Furthermore, the abnormal and all zero bands should be removed to ensure the validity of the algorithm. Therefore, 188 bands of the all 224 bands are used in the experiments. In the following experiments, the two datasets are denoted as Cuprite1 and Cuprite2, meanwhile, the 40th band as an example is shown in Figure 2.



(a) Cuprite1



(b) Cuprite2

Figure 2. Original image (the 40th band)

As a primary measure of reconstruction quality, the peak signal-to-noise (PSNR) of the reconstructed image is calculated to evaluate the performance of different reconstruction algorithms. The PSNR measured in dB is defined as,

$$\text{PSNR}(\mathbf{x}, \hat{\mathbf{x}}) = 20 \log_{10} \frac{\max(\mathbf{x})}{\sqrt{\text{MSE}(\mathbf{x}, \hat{\mathbf{x}})}} \quad (14)$$

where  $\mathbf{x}$  and  $\hat{\mathbf{x}}$  are the original and reconstructed image,  $\max(\mathbf{x})$  is the peak value of  $\mathbf{x}$ ,  $\text{MSE}(\mathbf{x}, \hat{\mathbf{x}})$  is the mean squared error,

$$\text{MSE}(\mathbf{x}, \hat{\mathbf{x}}) = \frac{1}{N} \|\mathbf{x} - \hat{\mathbf{x}}\|_2^2 \quad (15)$$

Figure 3 depicts the performance of 2DCS-SP compared with 2DCS without residual reconstruction. PSNR is averaged over all bands of two hyperspectral data. As expected, the residual reconstruction method with prediction from reconstruction of the key bands results in a significant performance



improvement for 2DCS-SP. In these graphs, the proposed method shows a great advantage even at lower sampling rates. The PSNR of method 2DCS-SP is up to 6dB higher than 2DCS at sampling rate  $SR = 0.5$ . The reconstructed images with different methods at sampling rate  $SR = 0.05$  are given in Figure 5. In the figure, the reconstructed images using the proposed 2DCS-SP has the higher PSNR than that of 2DCS, and has less visual error compared to the original image.

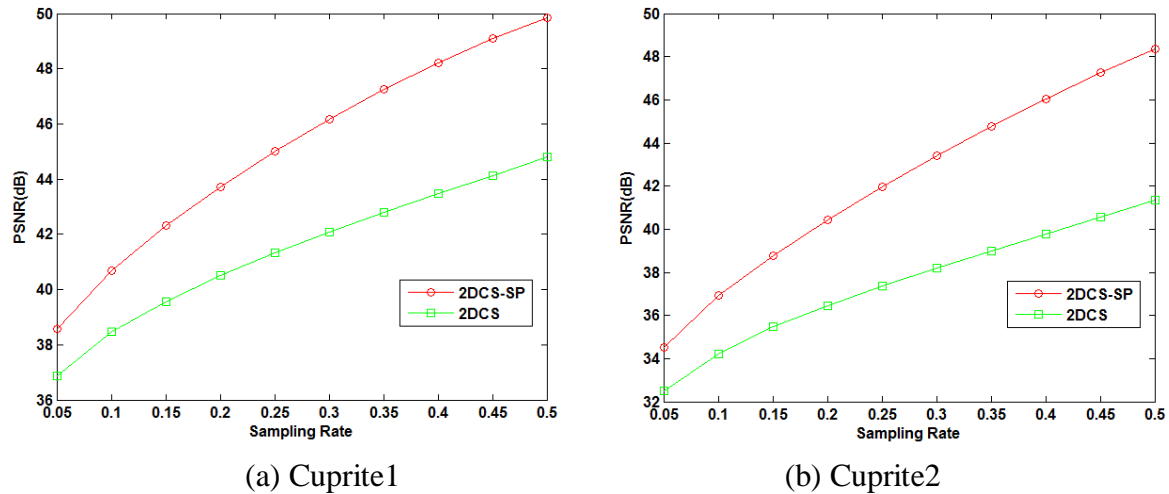


Figure 3. Comparison of method 2DCS-SP and 2DCS under different sampling rates.

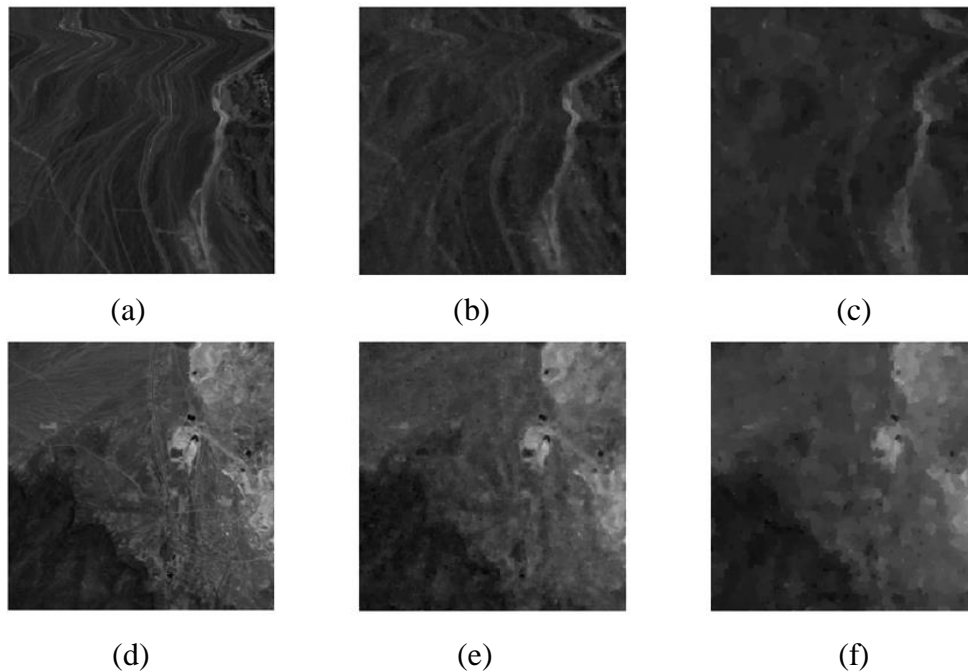


Figure 4. Reconstructed images with different methods at sampling rate 0.05. First row: (a) original image, (b) 2DCS-SP, PSNR = 38.0099 dB, (c) 2DCS, PSNR = 36.1068 dB. Second row: (d) original image, (e) 2DCS-SP, PSNR = 33.9578 dB, (f) 2DCS, PSNR = 32.0302 dB.

## 5. Conclusion

Since spatial correlation and spectral correlation are existed in hyperspectral images simultaneously, it is significant to exploit spectral correlation to improve reconstruction quality. In this paper, a residual reconstruct algorithm focused on hyperspectral images driven by two dimensional compressed sampling algorithm and spectral prediction between key and non-key band is proposed. Extensive experiment results demonstrate that the proposed residual reconstruction could obtain higher PSNR over 2DCS that does not utilize the spectral prediction in the reconstruction process.

The results demonstrate that the proposed method 2DCS-SP also outperforms 2DCS reconstruction in term of PSNR and visual quality.

## Acknowledgments

This work was supported by the National Natural Science Foundation of China (grant number 61901350); Scientific Research Plan Projects of Shaanxi Education Department (grant number 19JK0432) and Science Research Fund of Xi'an Aeronautics University (grant number 2019KY0208).

## References

- [1] NIU Y and WANG B. Extracting Target Spectrum for Hyperspectral Target Detection: An Adaptive Weighted Learning Method Using a Self-Completed Background Dictionary [J]. IEEE Transactions on Geoscience and Remote Sensing, 2017, 55(3): 1604-1617. DOI: 10.1109/TGRS.2016.2628085.
- [2] REN Z, WU L. Spectral-spatial Classification for Hyperspectral Imagery Based on Intrinsic Image Decomposition [J]. Spacecraft Recovery & Remote Sensing, 2019, 40(3): 111-120. DOI:10.3969/j.issn.1009-8518.2019.03.014.
- [3] CAI Q, LI E, JIANG J, et al. Study on the Tea Identification of Near-Infrared Hyperspectral Image Combining Spectra-Spatial Information [J]. Spectroscopy and Spectral Analysis, 2019, 39(08): 2522-2527.
- [4] CHEN S, ZHOU Y, QI R. Joint sparse representation of hyperspectral image classification based on kernel function [J]. Systems Engineering and Electronics, 2018, 40(3): 692-698. DOI: 10.3969 /j.issn. 1001-506X. 2018. 03. 31. (in Chinese)
- [5] FANG L, HE N, LI S, et al. A New Spatial-Spectral Feature Extraction Method for Hyperspectral Images Using Local Covariance Matrix Representation [J]. IEEE Transactions on Geoscience and Remote Sensing, 2018, 56(6): 3534-3546. DOI: 10.1109/ TGRS.2018.2801387.
- [6] PAN L, LI H C, MENG H, et al. Hyperspectral Image Classification via Low-Rank and Sparse Representation with Spectral Consistency Constraint [J]. IEEE Geoscience and Remote Sensing Letters, 2017, 14(11): 2117-2121.
- [7] TANG Z, FU G, CHEN J, et al. Low-rank Structure Based Hyperspectral Compression Representation [J]. Journal of Electronics & Information Technology, 2016, 38(05): 1085-1091.
- [8] K. Guo, X. Xie, X. Xu and X. Xing. Compressing by Learning in a Low-Rank and Sparse Decomposition Form [J]. IEEE Access, vol. 7, pp. 150823-150832, 2019.
- [9] WANG Z, FENG W, NIAN Y. Compressive- sensing-based lossy compression for hyperspectral images using spectral unmixing [J]. Infrared and Laser Engineering, 2018, 47(S1): 197-204.
- [10] Fowler J E and Du Q. Reconstructions from Compressive Random Projections of Hyperspectral Imagery [M]. In Optical Remote Sensing: Advances in Signal Processing and Exploitation Techniques, edited by Prasad S., Bruce L. M., and Chanussot J, Berlin: Springer Berlin Heidelberg, 2013: 31-48.
- [11] Xu Y, Wu Z, Chanussot J, et al. Joint Reconstruction and Anomaly Detection from Compressive Hyperspectral Images Using Mahalanobis Distance-Regularized Tensor RPCA [J]. IEEE Transactions on Geoscience and Remote Sensing, 2018, 56(5): 2919-2930.
- [12] Yin J, Sun J, and Jia X. Sparse Analysis Based on Generalized Gaussian Model for Spectrum Recovery with Compressed Sensing Theory [J]. IEEE Journal of Selected Topics in Applied Earth Observations and Remote Sensing, 2015, 8(6): 2752-2759.
- [13] Giampouras P V, Themelis K E, Rontogiannis A A, et al. Simultaneously Sparse and Low-Rank Abundance Matrix Estimation for Hyperspectral Image Unmixing [J]. IEEE Transactions on Geoscience and Remote Sensing, 2016, 54(8): 4775-4789.
- [14] WANG L, FENG Y. Compressed Sensing Reconstruction of Hyperspectral Images Based on Spatial-spectral Multihypothesis Prediction [J]. Journal of Electronics & Information Technology, 2015, 37(12): 3000-3008.
- [15] Liu H, Li Y, Xiao S, et al. Distributed Compressive Hyperspectral Image Sensing [C]. IEEE Sixth International Conference on Intelligent Information Hiding and Multimedia Signal Processing, Darmstadt, DE, Oct. 15-17, 2010: 607-610.

- [16] Li Wang, Yan Feng. "Hyperspectral Imaging via Three-dimensional Compressed Sampling", International Conference on Advanced Computer Science and Electronics Information (ICACSEI 2013), 355-359, Beijing, China, July 2013.
- [17] Feng, Y., Y. Jia, Y. Cao, and X. Yuan. "Compressed Sensing Projection and Compound Regularizer Reconstruction for Hyperspectral Images." *Acta Aeronautica et Astronautica Sinica*, 2012, 33(8): 1466-1473.
- [18] James E. Fowler, Sungkwang Mun, and Eric W. Tramel. "Multiscale block compressed sensing with smoothed projected Landweber reconstruction". *Proceedings of the European Signal Processing Conference*, Barcelona, Spain, August 2011.
- [19] W. Yin, S. P. Morgan, J. Yang, and Y. Zhang. "Practical compressive sensing with toeplitz and circulant matrices". *Rice University CAAM Technical Report TR10-01*, (2010).

## Biographies



**Li Wang** received the B.E. degree in electronic and information engineering from Xi'an University of Architecture and Technology, Xi'an, China, in 2009 and the M.S. degree in signal and information processing from Beihang University, Beijing, China, in 2012. She received the Ph.D. degree from Northwestern Polytechnical University, Xi'an, China, in 2018. She now is a lecturer in Xi'an Aeronautics University. Her research interests include compressed sampling, hyperspectral image processing, and optimization algorithm.



**Wei Wang** received the B.E. degree in electronics and information technology, the Master's degree in aerospace propulsion theory and engineering and the Ph.D. degree in electronic science and technology from the Northwestern Polytechnical University, Xi'an, China. Since 2015, he has been a lecturer in Xi'an Aeronautics University. His current research interests include antenna and radome design, electromagnetic scattering analysis and intelligent optimization algorithm.



**Boni Liu** received the B.E. degree in Technique of Measuring Control and Instrument from Xi'an Shiyou University, Xi'an, China, in 2003 and the M.S. degree in geodesy and engineering major from Xi'an University of Science and Technology, Xi'an, China, in 2006. Since 2006, she has been a lecturer in Xi'an Aeronautics University. Her research interests include communication technology and electronic measurement.